A chromatographic network for the purification of detergent-solubilized six-transmembrane epithelial antigen of the prostate 1 from *Komagataella pastoris* mini-bioreactor lysates

J Barroca-Ferreira [a,b,c], AM Gonçalves [a,b,c], MFA Santos [b,c], T Santos-Silva [b,c], CJ Maia [a], LA Passarinha [a,b,c,d,∗]

[a] CICS-UBI – Health Sciences Research Centre, University of Beira Interior, 6201-506 Covilhã, Portugal
[b] Associate Laboratory i4HB - Institute for Health and Bioeconomy, NOVA School of Science and Technology, Universidade NOVA de Lisboa, 2829-516 Caparica, Portugal
[c] UCIBIO – Applied Molecular Biosciences Unit, Department of Chemistry, NOVA School of Science and Technology, Universidade NOVA de Lisboa, 2829-516 Caparica, Portugal
[d] Laboratório de Fármaco-Toxicologia - UBIMedical, University of Beira Interior, 6201-284 Covilhã, Portugal

A R T I C L E   I N F O

A B S T R A C T

The Six-Transmembrane Epithelial Antigen of the Prostate 1 (STEAP1) is an integral membrane protein involved in cellular communications, in the stimulation of cell proliferation by increasing Reactive Oxygen Species levels, and in the transmembrane-electron transport and reduction of extracellular metal-ion complexes. The STEAP1 is particularly over-expressed in prostate cancer, in contrast with non-tumoral tissues and vital organs, contributing to tumor progression and aggressiveness. However, the current understanding of STEAP1 lacks experimental data on the respective molecular mechanisms, structural determinants, and chemical modifications. This scenario highlights the relevance of exploring the biosynthesis of STEAP1 and its purification for further bio-interaction and structural characterization studies. In this work, recombinant hexahistidine-tagged human STEAP1 (rhSTEAP1-His$_6$) was expressed in *Komagataella pastoris* (*K. pastoris*) mini-bioreactor methanol-induced cultures and successfully solubilized with Nonidet P-40 (NP-40) and n-Decyl-β-D-Maltopyranoside (DM) detergents. The fraction capacity of Phenyl-, Butyl-, and Octyl-Sepharose hydrophobic matrices were evaluated by manipulating the ionic strength of binding and elution steps. Alternatively, immobilized metal affinity chromatography packed with nickel or cobalt were also studied in the isolation of rhSTEAP1-His$_6$ from lysate extracts. Overall, the Phenyl-Sepharose and Nickel-based resins provided the desired selectivity for rhSTEAP1-His$_6$ capture from NP-40 and DM detergent-solubilized *K. pastoris* extracts, respectively. After a polishing step using the anion-exchanger Q-Sepharose, a highly pure, fully solubilized, and immunoreactive 35 kDa rhSTEAP1-His$_6$ fraction was obtained. Altogether, the established reproducible strategy for the purification of rhSTEAP1-His$_6$ paves the way to gather additional insights on structural, thermal, and environmental stability characterization significantly contributing for the elucidation of the functional role and oncogenic behavior of the STEAP1 in prostate cancer microenvironment.

1. Introduction

The Six-Transmembrane Epithelial Antigen of the Prostate 1 (STEAP1) is an integral six-transmembrane protein connected by intra- and extracellular loops located in tight- and gap-junctions, cytoplasm, and endosomal membranes [1]. The STEAP1 is over-expressed in prostate cancer (PCa), in contrast with non-tumoral tissues and vital organs, which may indicate a particular specificity for cancer microenvironments [2]. According to amino-acid sequence, transmembrane topology, and cellular localization, it was hypothesized that STEAP1 has a crucial role in cell-cell communications as a transporter protein [3] and in the stimulation of cell growth upon the increment of the intracellular levels of Reactive Oxygen Species [4]. Nevertheless, full-length human STEAP1 was produced in mammalian Human Embryonic Kidney (HEK)-

293 cells and the structure-function analysis of antibody-fragment bound STEAP1 (6Y9B, 2.97 Å resolution) through cryogenic Electron Microscopy (cryo-EM) techniques revealed a trimeric arrangement of the protein, suggesting a functional role in heterodimeric assembles with other STEAP1 counterparts [5,6]. This structural rearrangement supports the biological behavior of heme-binding site to recruit and orient intracellular electron-donating substrates to enable transmembrane-electron transport and the consequent reduction of extracellular metal-ion complexes. From a clinical perspective, the STEAP1 is one of the most relevant member of the STEAP family of proteins [7]. Indeed, several studies with monoclonal antibodies attached to radioisotopes demonstrated promising results in targeting and monitoring STEAP1 expression and in controlling PCa progression [8,9]. Moreover, *in vitro* and *in vivo* studies showed that STEAP1-derived peptides are immunogenic and suitable for cytotoxic T lymphocytes recognition [10,11], which indicate a potential use towards anti-cancer vaccines development. These data highlight the usefulness of STEAP1 as a potential promising tool as a biomarker or a target for anti-cancer therapies. So far, monomeric STEAP1 high-resolution structures are not available highlighting the scarce of structural and functional knowledge on the protein and preventing to understand its biological role in PCa. In fact, the lack of structural data is also verified in the other STEAP family members with a total of four deposited structures in the Protein Data Bank (PDB): two crystal structures of the membrane-proximal oxidoreductase domain of human STEAP3 (2VNS, 2 Å resolution and 2VQ3, 2 Å resolution) [12] and two cryo-EM structures of human STEAP4 domains (6HD1, 3.8 Å resolution and 6HCY, 3.1 Å resolution) [13]. To decipher the molecular interactions between STEAP1 and highly specific antagonist drugs capable of blocking its oncogenic effects, a complete structural characterization of the protein is demanded. Nevertheless, the major downsides associated with structure-based design studies relies on attaining high amounts of the target protein with substantial purification yields. In order to overcome these issues, our research team recently proposed an optimized fermentation strategy to improve the biosynthesis and stabilization of biologically active recombinant hexahistidine-tagged human STEAP1 (rhSTEAP1-His$_6$) in a mini-bioreactor *Komagataella pastoris* (*K. pastoris*) X-33 Mut$^+$ cultures upon the application of a glycerol gradient fed-batch profile associated with a methanol constant feed with 6 % (v/v) DMSO and 1 M Proline supplementation [14]. Thereafter, a suitable isolation strategy should be designed and optimized. To date, there are only two studies focusing on the isolation of recombinant STEAP1, produced in both HEK and Baculovirus-Insect cells using Immobilized Metal Affinity Chromatography (IMAC) followed by Size Exclusion Chromatography (SEC) [5,6]. Additionally, a recent pioneer experimental research explored the purification of the human native paralog of STEAP1 protein, naturally overexpressed in neoplastic PCa cell line, by Hydrophobic Interaction Chromatography (HIC) as capture step and further polishing using a Co-Immunoprecipitation approach [15]. Despite promising steps were given in the discovery of a biotechnology procedure for handling both native and recombinant STEAP1 protein, these studies present several limitations that may compromise their application for the generation of high-quality recombinant proteins. When used as expression platforms, mammalian cells may produce low expression levels and yields, toxic target when overexpressed, difficult to scale-up, and time consuming for expression and optimization; while for insect cells, it is observed a possibility of misfolding, aggregation, or cell lysis, also time consuming for expression and optimization, and simplified *N*-glycosylation [16]. In this sense, microbial platforms share attractive features in protein discovery and has gained attention in biotechnology field as efficient production tool. From this class, *K. pastoris* is the preferred system for the large-scale production of eukaryotic proteins, once it has i) high similarity with

advanced eukaryotic expression systems, ii) easy and stable integration of foreign genes into their genome, iii) cost-effective cultivation cultures, iv) scale-up capacity in large fermentations, v) fast growth rate and increased cell densities platforms, vi) sophisticated eukaryotic post-translational modifications due to strong and tightly regulated promoters, vii) proteolytic processing and folding, and [8] cellular translocation and trafficking mechanisms [17,18]. Independently on the diverse purification strategies already reported, the expression host system could be responsible for distinct structural rearrangements and conformations of the protein under study, which will trigger a different chromatographic behavior. Therefore, it is quite imperative to implement novel and alternative approaches for the isolation of the recombinant human STEAP1 protein, with increased degree of purity, high quality of protein sample, and concentration compatible with mainstream biophysical and structural determination techniques. Altogether, these facts encouraged the development of an integrated strategy considering the i) increased hydrophobic nature of the STEAP1 protein, the ii) hexahistidine-tagged tail residues, and the iii) basic isoelectric point (pI), which contrast with the acidic pI of most heterologous proteins from *K. pastoris* for the solubilization and purification of stable, biologically active, and pure amounts of rhSTEAP1-His$_6$. To attain this goal, in-house and commercial detergent kits were initially screened and compared to evaluate their efficiency to recover and solubilize an active form of rhSTEAP1-His$_6$ from *K. pastoris* extracts. The target protein was purified using a combined two-step procedure – HIC and IMAC – as main capture steps followed by Anion Exchange Chromatography (AEX) as a final polishing step. The strategy here established represents a novelty in the purification of rhSTEAP1-His$_6$ using traditional chromatography strategies and fulfills all the conditions need to obtain a rhSTEAP1-His$_6$ fraction with tailored improved stability, biological activity, purity, and concentration, when compared to previously reported approaches. Altogether, these findings are crucial for undertaking further structural and functional characterization studies using pure fractions of rhSTEAP1-His$_6$.

2. Materials and methods

2.1. Chemicals

Ultrapure reagent-grade water was obtained with a Mili-Q system (Milipore/Waters). Zeocin^{TM} was acquired from InvivoGen (Toulouse, France). Yeast nitrogen base was bought from Pronadisa (Madrid, Spain). Glycerol was obtained from HiMedia Laboratories (Mumbai, India). Peptone was purchased from BD (Franklin Lakes, NJ, USA). Biotin was bought from Hoffmann-LaRoche (Basel, Switzerland). Genapol X-100 and Digitonin were obtained from Merck (Darmstadt, Germany). Glucose, agar, yeast extract, dimethyl sulfoxide (DMSO), phosphoric acid, glass beads (500 μm diameter), Triton X-100 and Tween-20 were purchased from ThermoFisher Scientific (Loughborough, UK). Ammonium sulfate ((NH_4)$_2SO_4$), Proline and Sodium Dodecyl Sulfate (SDS) were acquired from PanReac Applichem (Darmstadt, Germany). Tris-base was bought from Fisher Scientific (Epson, UK). Nonidet P-40 (NP-40) was obtained from Fluka (Monte Carlo, Monaco). Popular Detergent Kit was acquired by Anatrace (Maumee, OH, USA). Bis-Acrylamide/Acrylamide 40 % and GRS Protein Marker MultiColour was purchased from GRiSP Research Solutions (Oporto, Portugal). All chemicals used were of analytical grade, commercially available, and used without further purification.

2.2. Recombinant hSTEAP1-His6 production

The rhSTEAP1-His$_6$ biosynthesis was performed using *K. pastoris* X-33 Mut$^+$ harboring the expression construct pPICZαB-hSTEAP1-

His$_6$, as previously reported [14]. Briefly, cells were grown at 30 ºC in YPD plates (1 % yeast extract, 2 % peptone, glucose and agar, and 200 µg mL^{-1} Zeocin), and a single colony was used to inoculate BMGH medium (100 mM potassium phosphate buffer at pH 6.0, 1.34 % yeast nitrogen base, 4×10^{-4} g L^{-1} biotin, 1 % glycerol and 200 µg mL^{-1} Zeocin). Then, cells were grown at 30 ºC and 250 rpm until the cell density at 600 nm (OD$_{600}$) typically reached 6. This culture was used to inoculate the modified basal salts medium (BSM) containing 4.35 mL L^{-1} trace metal solution (SMT) with an initial OD$_{600}$ of 0.5. The fermentation process was carried out in a mini-bioreactor platform under constant methanol/gradient glycerol feeding for 10 h, upon induction with 6 % (v/v) DMSO and 1 M Proline for STEAP1 stabilization. The pH and temperature were kept constant throughout batch and fed-batch modes at 4.7 and 30 ºC, respectively, while glycerol gradient and methanol constant feeding strategies were controlled by IRIS Software (Infors HT, Switzerland). The cells were harvested by centrifugation for 10 min at 1500 g and 4 ºC, and store at – 20 ºC until further use.

2.3. Cell lysis and rhSTEAP1-His$_6$ recovery

The *K. pastoris* crude was disrupted in lysis buffer (50 mM Tris-Base buffer at pH 7.8 and 150 mM NaCl) supplemented with protease inhibitors cocktail (Roche, Basel, Switzerland), followed by enzymatic digestion with 1 mg mL^{-1} Lysozyme (Merck, Darmstadt, Germany) incubation for 15 min at room temperature. The mixture was vortexed 7 times in 1 min intervals between glass beads and ice, and then centrifuged at 500 g for 5 min at 4 ºC to remove cell debris. The supernatant (S500) was collected while the pellet (P500) was resuspended in lysis buffer complemented with 1 mg mL^{-1} DNase I (PanReac Applichem, Darmstadt, Germany) and further centrifuged at 16000 g for 30 min at 4 ºC. The supernatant (S16000) was collected while the pellet (P16000) was resuspended in chromatographic equilibrium buffer (HIC: 50 mM (NH$_4$)$_2$SO$_4$ in 10 mM Tris-Base buffer at pH 7.8 plus 0.1 % (v/v) NP-40; IMAC: 500 mM NaCl in 50 mM Tris-Base buffer at pH 7.8, plus 5 mM Imidazole and 0.1 % (v/v) *n*-Decyl-β-D-Maltopyranoside (DM)) at 4 ºC until full solubilization [19]. The quantification of the total amount of protein was measured using Pierce^{TM} BCA Protein Assay Kit (ThermoFisher Scientific, Loughborough, UK).

2.4. Detergent screening for rhSTEAP1-His$_6$ solubilization

The rhSTEAP1-His$_6$ solubilization studies were performed in the P16000 fraction obtained from *K. pastoris* lysis, upon complete resuspension in solubilization buffer (lysis buffer plus 0.1 % (v/v) detergent) overnight at 4 ºC with constant stirring ($\sim$ 40 mg mL^{-1} total protein concentration) (Table 1). In these experiments, the pellets P16000 were resuspended in the respective solubilization buffer, and a control extract without detergent was also performed.

2.5. Purification of rhSTEAP1-His$_6$ solubilization

The purification trials were performed in an ÄKTA Avant system with UNICORN 6.1 software (Cytiva, Malborough, MA, USA) at room temperature. All buffers were filtered through a 0.22 μm pore size membrane, ultrasonically degassed. Butyl-Sepharose^{TM} HP (10 mL), Octyl-Sepharose^{TM} 4FF (10 mL), HiTrap^{TM} Phenyl HP (5 mL), HisTrap^{TM} FF (5 mL), and HiTrap^{TM} Q FF (5 mL) (Cytiva, Malborough, MA, USA), were used as HIC, IMAC, and AEX stationary phases, respectively. The HiTrap^{TM} Phenyl HP (5 mL) was initially equilibrated with 50 mM (NH$_4$)$_2$SO$_4$ in 10 mM Tris-Base buffer at pH 7.8 supplemented with 0.1 % (v/v) NP-40, and rhSTEAP1-His$_6$ samples (1 mL with a total protein concentration of 40 mg mL^{-1}) was loaded onto the column at a flow rate of 0.5 mL min^{-1}. After elution of the unretained species, an elution step at 10 mM

Tris-Base buffer at pH 7.8 was applied, followed by a linear gradient from 10 mM Tris-Base buffer at pH 7.8 to H$_2$O, both at 1.0 mL min^{-1}. The HisTrap^{TM} FF (5 mL) packed with nickel and cobalt ions were equilibrated with 500 mM NaCl in 50 mM Tris-Base buffer at pH 7.8 supplemented with 0.1 % (v/v) DM. Similar to HIC strategy, rhSTEAP1-His$_6$ samples (1 mL with a total protein concentration of 40 mg mL^{-1}) was loaded onto the column at a flow rate of 0.5 mL min^{-1}. After elution of the unretained species, an imidazole stepwise elution gradient (10, 50, 175, 300, and 500 mM) was applied at 1.0 mL min^{-1}. Subsequently, both the HIC fraction obtained with 10 mM Tris-Base buffer at pH 7.8 and the IMAC fraction recovered in 175 mM Imidazole step were injected in HiTrap^{TM} Q FF, used as a final polishing step, previously equilibrated with 10 mM Tris-Base buffer at pH 10.0. After elution of unretained species, NaCl concentration was increased in a stepwise mode to 300 mM and 500 mM at pH 10.0, and 1 M at pH 7.8 in 10 mM Tris-Base buffer. The AEX buffers were supplemented with 0.1 % (v/v) NP-40 or DM, respectively for pre-purified samples obtained from HIC or IMAC. The pH, pressure, conductivity, and absorbance at 280 nm were continuously monitored throughout the entire chromatographic run. The fractions of interest were collected, desalted, and concentrated with Vivaspin concentrators (10,000 MWCO). The samples were further stored at 4 ºC for purity and immunoreactivity analysis. All procedures including the regeneration steps were carried out according to manufacturer's instructions (Cytiva, Malborough, MA, USA).

2.6. SDS-PAGE and western-blot

Reducing SDS-PAGE was carried out according to the method of Laemmli [20]. Samples were boiled for 5 min at 95 ºC and resolved in 12.5% (V/V) acrylamide gels at 120 V for approximately 2 h. Then, one gel was stained by Coomassie brilliant blue while the second gel was transferred into a polyvinylidene difluoride (PVDF) membrane (Cytiva, Malborough, MA, USA) at 750 mV for 90 min and 4 ºC. The membrane was blocked for 1 h in a 5 % (w/v) non-fat milk solution in TBS-T and incubated overnight with mouse anti-STEAP1 monoclonal antibody 1:300 (B-4, sc-271872, Santa Cruz Biotechnology, Dallas, TX, USA) at 4 ºC with constant stirring. Afterwards, membrane was incubated with goat anti-mouse IgGk BP-HRP 1:5000 (sc-516102, Santa Cruz Biotechnology, Dallas, TX, USA) for 2 h at room temperature with constant stirring. Finally, rhSTEAP1 immunoreactivity was visualized using ChemiDoc^{TM} MP Imaging System (Bio-Rad, Hercules, CA, USA) after a brief incubation with Clarity ECL Substrate (Bio-Rad, Hercules, CA, USA).

2.7. Total protein quantification

Quantification of the total amount of proteins was measured by Pierce^{TM} BCA Protein Assay Kit (Thermo Scientific, Loughborough, UK) using Bovine Serum Albumin (BSA) as standard and calibration control samples according to the manufacturer's instructions.

3. Results

3.1. Biosynthesis of rhSTEAP1-His$_6$ in Komagataella pastoris cultures

The rhSTEAP1-His$_6$ was produced in *K. pastoris* methanol-induced cultures using pPICZαB-rhSTEAP1 plasmid. Concerning the concentration levels of a typical 6 g crude extract of *K. pastoris* cultures, we obtained values of approximately 40 mg mL^{-1} of total protein. After a typical mini-bioreactor fermentation, the Western-Blot (WB) analysis revealed that immunologically active rhSTEAP1-His$_6$ protein was detected in its monomeric conformation of $\sim$ 35 kDa, as well as in high molecular weight isoforms of $\sim$ 48 and

Table 1

General characteristics of the detergents used for the rhSTEAP1-His$_6$ solubilization studies[1].

	Detergent	Detergent Type	Critical Micellar-Concentration (CMC) (mM)	Aggregation Number
In-house	Sodium Dodecyl Sulfate (SDS)	Ionic	7-10	62
	Triton X-100	Non-ionic	0.2-0.9	48-106
	Digitonin		<0.5	60
	Genapol X-100		0.15	88
	Nonidet P-40 (NP-40)		0.05-0.3	100-155
Anatrace Popular Detergent Kit	3-[(3-cholamidopropyl)dimethylammonio]-1-propanesulfonate (CHAPS)	Zwitterionic	8	10
	Fos-Choline-12 (FOS12)		1.5	54
	5-Cyclohexyl-1-pentyl-β-D-Maltoside (CYMAL-5)	Non-ionic	2.4–5.0	47
	n-Decyl-β-D-Maltopyranoside (DM)		1.8	69
	n-Dodecyl-β-D-Maltopyranoside (DDM)		0.17	78-149
	n-Octyl-β-D-Glucopyranoside (OG)		18-20	27-100

[1] Data obtained from Anatrace (Maumee, OH, USA: www.anatrace.com) and Merck (Darmstadt, Germany: www.merckgroup.com)

∼ 63 kDa, that may correspond to glycosylated or homo- or heterodimeric aggregates of rhSTEAP1 in agreement with the previously reported [14].

3.2. Detergent screening for rhSTEAP1-His$_6$ solubilization

In this work, we performed a detergent screening to determine the most suitable for the recovery of an active and fully solubilized fraction of human STEAP1, previously extracted from *K. pastoris* lysates, comparing the efficiency of an in-house detergent kit (SDS, Triton X-100, Digitonin, Genapol X-100, and NP-40) with the commercially available Popular Detergent Kit from Anatrace (CHAPS, CYMAL-5, DM, DDM, FOS12, and OG). The nature of each used detergent and their general features are summarized in Table 1. The performance of each detergent was measured by a direct densitometric comparison between rhSTEAP1-His$_6$ immunoreactive bands.

The results showed that rhSTEAP1-His$_6$ extraction was increased by NP-40 followed by Genapol X-100 and Digitonin, with the in-house detergent kit (Figure 1A). On the opposite plan, SDS and Triton X-100 reveal to be ineffective in the solubilization of rhSTEAP1-His$_6$, presenting a similar profile to control experiment with evidence of protein degradation. Concerning the commercial kit, the solubilization of rhSTEAP1-His$_6$ was more efficient with DM (reduced amounts of degraded rhSTEAP1-His$_6$), followed by CYMAL-5 (Figure 1B). Despite all the tested detergents (except DDM in which an immunoactive protein fraction was not detected) were able to fully solubilize the monomeric rhSTEAP1-His$_6$ with different minor levels of protein degradation, it should be emphasized that NP-40 and DM were the ones where the target protein was recovered in P16000 fraction with the expected molecular weight of ∼35 kDa with an increased WB qualitative densitometry.

3.3. HIC/IMAC and IEX Platform for rhSTEAP1-His$_6$ purification

The elution of the rhSTEAP1-His$_6$ mainly occurs directly in the flowthrough for Butyl- and Octyl-Sepharose trials along with significant amounts of endogenous proteins from the expression host. This indicate that under these binding conditions (50 mM $(NH_4)_2SO_4$ in 10 mM Tris-Base buffer at pH 7.8 plus 0.1% (v/v) NP-40), a major fraction of the target protein does not interact with the hydrophobic matrices hindering an efficient protein separation (Please see Supplementary Material). However, in case of Phenyl resin, high molecular weight isoforms of rhSTEAP1-His$_6$ of 48 and 63 kDa did not bind to the matrix and directly eluted in the flowthrough (Figure 2B, Peak I) while the immunologically active

monomeric isoform of rhSTEAP1-His$_6$ with 35 kDa was completely captured by the hydrophobic matrix during the binding phase and was mainly recovered in 10 mM Tris-Base elution step (Figure 2B, Peak II), with some losses observed during the linear gradient to H_2O (Figure 2B, Peak III).

In parallel, IMAC experiments were also conducted. In the trials with cobalt, rhSTEAP1-His$_6$ is directly eluted in the flowthrough revealing that under the binding conditions (500 mM NaCl in 50 mM Tris-Base buffer at pH 7.8 plus 0.1% (v/v) DM), the hexahistidine-tag of the target protein does not interact with the metal ion of the chromatographic resin (Please see Supplementary Material). By the contrary, in the nickel-charged IMAC resin, a partial retention of rhSTEAP1-His$_6$ to the matrix throughout the binding phase was observed (Figure 3A and 3B, Peak I). Despite minor amounts of rhSTEAP1-His$_6$ were observed in the 10 and 50 mM imidazole step gradients, the monomeric protein isoform (35 kDa) was mainly eluted in the 175 mM imidazole step, together with traces of high molecular weight isoforms of 48 kDa (Figure 3A and 3B, Peak III).

Upon the analysis of the SDS-PAGE gel, the purity level of the rhSTEAP1-His$_6$ samples obtained from both HIC and IMAC strategies is considerably low, due to an increased amount of co-eluting proteins, demanding a polishing stage with the anion exchanger Q-Sepharose as a final purification step [21]. Briefly, the SDS-PAGE and WB results from the polishing of rhSTEAP1-His$_6$ pre-purified fraction from HIC demonstrated that immunologically active target protein was preferentially eluted with 300 and 500 mM NaCl (Figure 4A and 4B, Peaks III and IV, respectively), despite residual losses in the flowthrough, with the last one revealing an acceptable purity level.

Curiously, the SDS-PAGE and WB analysis of the polishing step of rhSTEAP1-His$_6$ pre-purified fraction from IMAC confirmed the tendency of the protein to be mainly eluted with 500 mM NaCl (Figure 5A and 5B, Peak II) exhibiting a considerable high degree of purity, although residual losses of the target were observed in the final step with 1 M NaCl (Figure 5B, Peak III) which is mainly responsible for the elution of the expression host proteins.

4. Discussion

Membrane Proteins (MPs) play key roles in several cellular functions representing more than 50 % of therapeutic targets currently available in the market. Regardless their value, MPs represent less than 2% of the deposited structures in the PDB (https://www.rcsb.org/, (accessed on 14th June 2022). Therefore, the structural and funcional characterization of these proteins could pro-
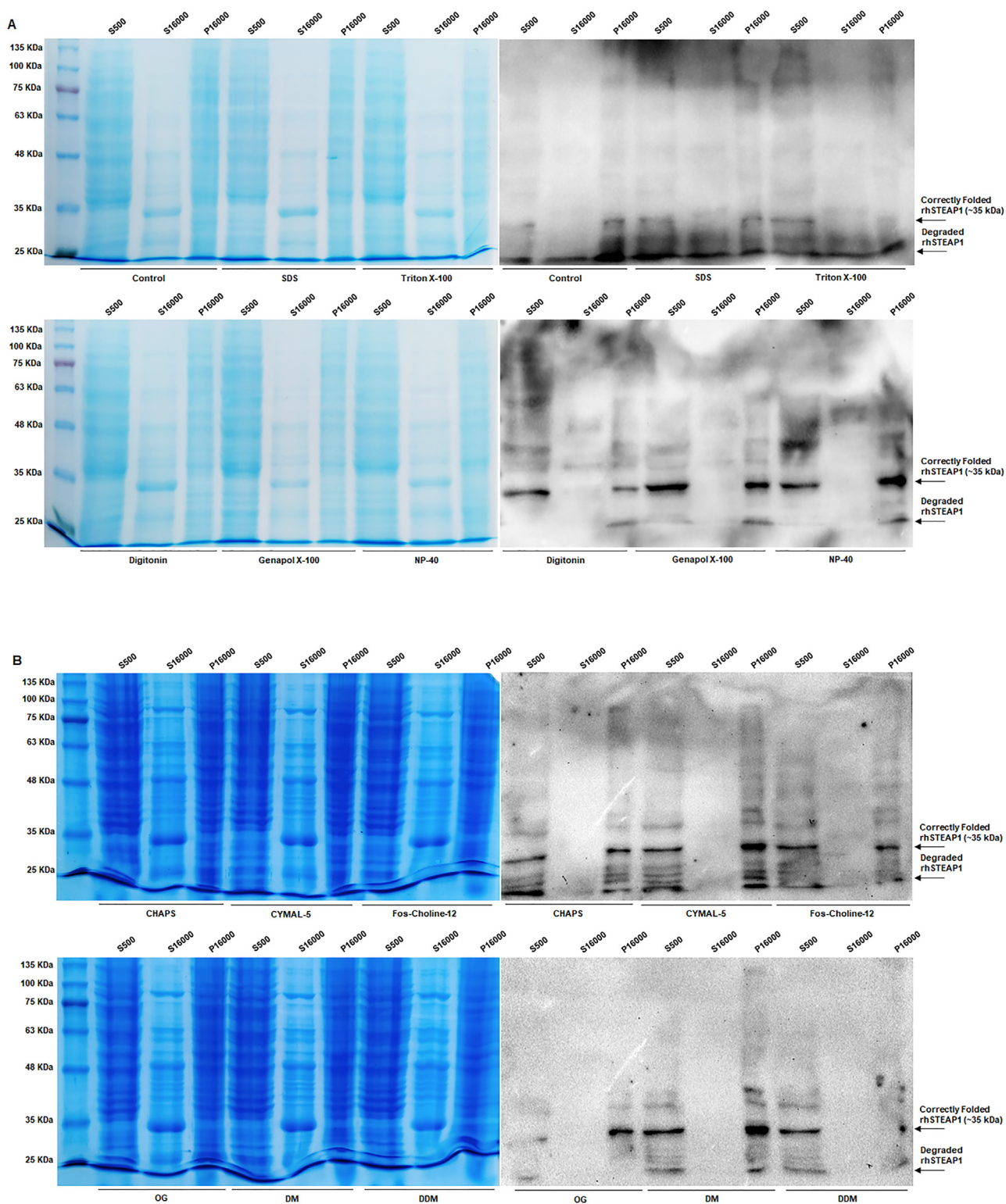
Fig. 1. SDS-PAGE and WB analysis of the performance of different detergents from an in-house detergent kit (A) and Anatrace Popular Detergent Kit (B) in solubilizing rhSTEAP1-His$_6$ from *K. pastoris* crude extracts upon two centrifugation steps at 500 g and 16000 g.

vide details on their mechanisms of action, which is crucial for the design of novel highly-effective drugs. Taking into considering the usefulness of STEAP1 as a promising therapeutic agent against PCa, it is crucial to established a biotechnology platform for its biosynthesis, extraction, and purification with the final purpose of obtaining a high-resolution 3D structure of the protein. Despite few

attemps with both recombinant and native isoforms of STEAP1, experimental structural data is barely scarce (Table 2).

The success of structural-based trials striclty depends on obtaining high amounts of pure, active, and stable protein. To achieve such goal, novel integrative approaches including high-throughput screens of solubilization conditions and highly selective chromato-

Table 2

Integrative overview of existent strategies from the biosynthesis to the purification of STEAP1 towards structural resolution studies (n.a. – not applicable).

Protein	ExpressionSystem	Extraction	Isolation Flowchart	Final Sample Buffer	Structural Resolution	Ref.
Recombinant Human STEAP1	*Komagataella pastoris*	Ordinary Lysis Buffer (150 mM NaCl, 50 mM Tris, 0.1% DM pH 7.8)	Immobilized Metal Affinity Chromatography (Nickel) *(A)* Ion Exchange Chromatography (Q-Sepharose) *(B)*	500 M NaCl, 10 mM Tris, 0.1% NP-40, pH 10.0	n.a.	This Work
Recombinant Human STEAP1	*Komagataella pastoris*	Ordinary Lysis Buffer (150 mM NaCl, 50 mM Tris, 0.1% NP-40 pH 7.8)	Hydrophobic Interaction Chromatography (Phenyl-Sepharose) *(A)* Ion Exchange Chromatography (Q-Sepharose) *(B)*	500 M NaCl, 10 mM Tris, 0.1% NP-40, pH 10.0	n.a.	This Work
Native Human STEAP1	Neoplastic Prostate Cancer Cells (LNCaP)	RIPA Buffer (50 mM Tris, 150 mM NaCl, 1 mM EDTA, 0.5% Sodium Deoxycholate, 0.1% SDS, 1% NP-40, pH 7.8)	Hydrophobic Interaction Chromatography (Butyl-Sepharose) coupled to Co-Immunoprecipitation	10 mM Tris pH 7.8	n.a.	[15]
Recombinant Human STEAP1	Human Embryonic Kidney Cells (HEK)	Ordinary Lysis Buffer (50 mM Tris, 250 mM NaCl, 0.7% digitonin, 0.3% n-Dodecyl-β-D-Maltoside, 0.06% Cholesteryl hemi-succinate, pH 7.8)	Affinity Chromatography (Streptactin) *(A)* Size Exclusion Chromatography (Superdex 200 10/300) *(B)*	20 mM Tris, 200 mM NaCl, 0.08% Digitonin, pH 7.8	~3.0 Å Cryo-EM structure of trimeric human STEAP1 bound to three antigen-binding fragments of mAb 120.545 (PDB 6Y9B)	[5]
Recombinant Rabbit STEAP1	*Baculovirus-Insect Cells*	Ordinary Lysis Buffer (200 mM HEPES, 150 mM NaCl, 1 mM PMSF, 5 mM MgCl$_2$, 5 mM Imidazole, 10 μM hemin chloride, 1.5% MNG-DDM, pH 7.5)	Affinity Chromatography (Talon Co^{2+}) *(A)* Size Exclusion Chromatography (Superdex 200 10/300) *(B)*	20 mM HEPES, 150 mM NaCl, 0.01% MNG-DDM, pH 7.5	n.a.	[6]

graphic strategies must be developed. Despite the challenges in handling MPs, over the last few years, our research group was focused on the tailor-made optimization of up- and down-stream processing conditions of this class of biomolecules [15,19,22-24]. In this work, encouraged by our previous efforts [14], we propose to increase the final biosynthesis yield of the human STEAP1 recombinantly produced rhSTEAP1-His$_6$ in *K. pastoris* methanol-induced cultures using a mini-bioreactor fermentation. When compared to the production of the native form of human STEAP1 [15], the concentration of the recombinant protein increased in an nearly 4-fold ratio from 12 mg mL^{-1} to 40 mg mL^{-1}.

A second challenge presented by MPs is the respective extraction from their lipid bilayer native environment. Detergents are amphipathic molecules containing a polar head group and long hydrocarbon chain capable to dissolute membranes and solubilize functional integral MPs by mimicking the natural lipid bilayer and consequently to prevent protein denaturation and aggregation [25]. The choice of a suitable detergent should promote a highest efficiency of extraction but also to ensure that target protein maintain their native and stabilized form [25]. Nevertheless, it should be reinforced that the most suitable condition for solubilization is not often the condition that extracts the largest amount of MPs. Generally, ionic detergents are harsh and not ideal for MPs solubilization once the extracted proteins typically undergo a complete loss of function as a result of degradation and unfolding [26,27]. This behavior was observed in the rhSTEAP1-His$_6$ solubilization with SDS, in which the target protein showed evidence of degradation in low molecular weight counterparts, in a similar profile to control ex-

periment (Figure 1A). Moreover, with few exceptions, zwitterionic detergents such as Fos-Choline-12 and CHAPS are more suitable for MPs solubilization rather than ionic class [27]. Fos-Choline-based detergents readily extract MPs but usually in an inactive and misfolded state [28] despite CHAPS is useful at minimizing the denaturation of MPs, the interaction between this agent and MPs are too weak to be effective at preventing protein aggregation [27]. As referred in literature for several other MPs, although Fos-Choline-12 could be an efficient solubilizing agent, these biomolecules are repeatedly recovered in an inactive form; Also, it is unlikely that CHAPS solubilized sample have utility for MPs structural studies, and therefore both detergents were then discarded for further trials [28,29]. Zwitterionic detergents with charged groups tend to be harsh in solubilizing MPs and are generally more deactivating that mild detergents containing large sizes of the head group and long length of the alkyl chain such as non-ionic detergents which are nowadays the most used class for the solubilization of a wide variety of MPs, particularly G-protein coupled receptors (GPCRs) and ion channels, in their active states [29,30]. Indeed, the results demonstrated that rhSTEAP1-His$_6$ solubilization was highly effective using non-ionic detergents, when compared to ionic and zwitterionic, in both in-house and commercial kits. Regarding the in-house detergent kit, the solubilization of the target protein was more effective upon Digitonin, Genapol X-100, and NP-40 supplementation (Figure 1A). From these, Digitonin is preferentially used in protein interaction studies and in combination with other detergents for extraction since it is not able to effectively solubilize MPs, mainly due to its mild nature which tends to preserve mild inter-
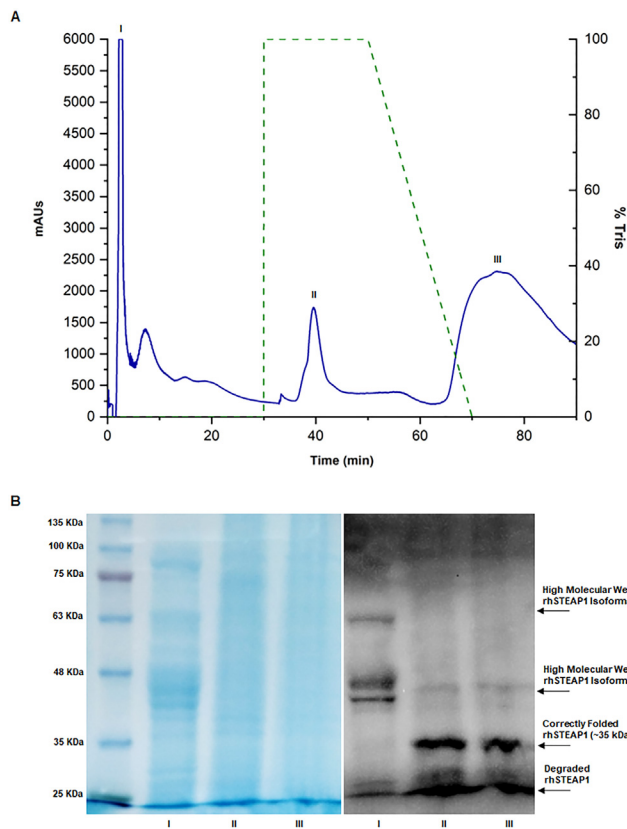
Fig. 2. (A) Chromatographic profile of rhSTEAP1-His$_6$ purification on HiTrap™ Phenyl HP from K. pastoris solubilized membranes. Blue line represents absorbance at 280 nm. Peak I, adsorption performed at 50 mM (NH$_4$)$_2$SO$_4$ in 10 mM Tris-Base buffer at pH 7.8 + 0.1 % (v/v) NP-40 (0.5 mL min^{-1}); Peak II, desorption performed at 10 mM Tris-Base buffer + 0.1 % (v/v) NP-40 (1.0 mL min^{-1}); Peak III, desorption performed by a linear gradient between 10 mM Tris-Base buffer + 0.1 % (v/v) NP-40 to H$_2$O (1.0 mL min^{-1}). (B) SDS-PAGE and WB analysis depicted for each peak.

Fig. 3. (A) Chromatographic profile of rhSTEAP1-His$_6$ purification on nickel-charged HisTrap™ FF crude from K. pastoris solubilized membranes. Blue line represents absorbance at 280 nm. Peak I, adsorption performed at 500 mM NaCl in 50 mM Tris-Base buffer at pH 7.8 + 0.1 % (v/v) DM (0.5 mL min^{-1}); Peak II, desorption performed at 10 mM Imidazole in 500 mM NaCl and 50 mM Tris-Base buffer at pH 7.8 + 0.1 % (v/v) DM (1.0 mL min^{-1}); Peak III, desorption performed at 175 mM Imidazole in 500 mM NaCl and 50 mM Tris-Base buffer at pH 7.8 + 0.1 % (v/v) DM (1.0 mL min^{-1}). (B) SDS-PAGE and WB analysis depicted for each peak.

actions between MPs [26]. Furthermore, and excepting Triton X-100, the results indicated a tendency between higher detergent aggregation number and increase efficiency in rhSTEAP1-His$_6$ solubilization in a biologically active and stable form (Table 1, Genapol X-100 aggregation number = 88; NP-40 aggregation number = 149). The analysis of the Anatrace Popular Detergent kit demonstrated that the solubilization of rhSTEAP1-His$_6$ was more efficient upon DM and CYMAL-5 supplementation (Figure 1B). OG, a small head-group short chain detergent, usually forms small protein-detergent complexes often leading to deactivation of MPs [27,29]. The detergents with a longer length of the alkyl chain provides greater ability to extract functionally active rhSTEAP1-His$_6$ such as the alkyl-glucosides DM and DDM [29]. Particularly, these maltoside-bearing conventional detergents have been demonstrating enhanced behaviors in preserving the native structure of a wide variety of MPs, inhibiting protein denaturation and aggregation [27]. Also, both DM and DDM are considered gentler detergents and have favorable properties for maintaining the functionality of more-aggregation-prone MPs in solution [30]. This fact can explain the successful application of DM for the solubilization of rhSTEAP1-His$_6$ is thought to be highly unstable. Interestingly, despite DDM has superior stabilization efficacy in terms of biologically active MPs, this detergent tends to form large protein-detergent complexes, which provide reduced amount of solubilized target protein and is unfavorable for MPs crystallization [27]. These findings justify the absence of immunoreactive domains of rhSTEAP1-His$_6$ in the WB analysis of DDM-solubilized fraction screening (Figure 1B). Although CYMAL-5 was apparently highly effective in the solubilization of

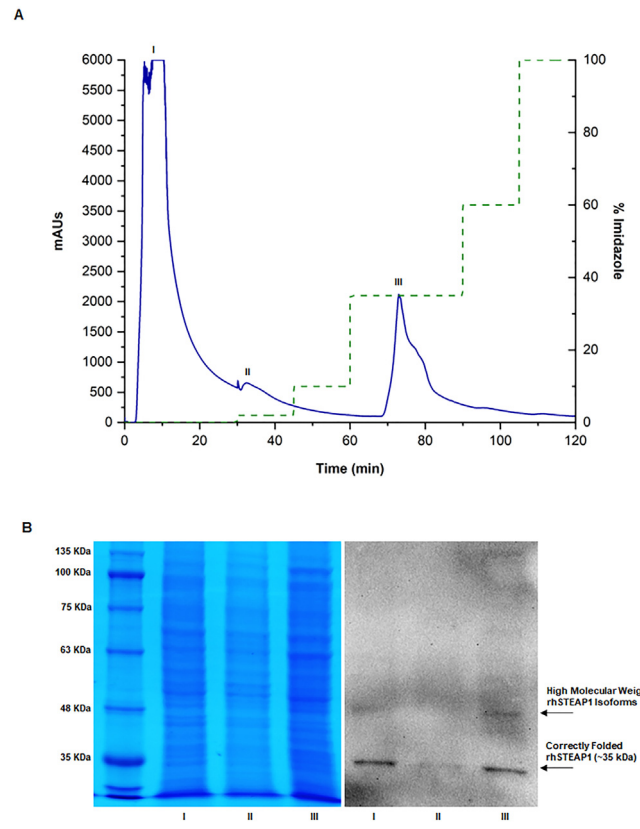the target protein, DM was able to reduce the amount of degraded rhSTEAP1-His$_6$ (Figure 1B) and has increased aggregation number (Table 1, CYMAL-5 aggregation number = 47; DM aggregation number = 69), which sustain the preferential use of this detergent.

In further protein purification steps, detergents play an essential role in maintaining the protein optimal environment being indispensable as chromatographic buffer supplements [31]. The isolation of MPs involves several sequential techniques that must explore their intrinsic properties. Considering the hydrophobic structural features of the rhSTEAP1-His$_6$, which presents six-transmembrane helices in the internal core and a 69 residue N-terminal intracellular tail as anchoring region [1], a highly specific interaction between the target protein and HIC matrices might be an appealing starting point. HIC is a widely used and powerful lab-scale purification approach which has been explored as an alternative for the purification of biomolecules and as a key step in downstream processing, often yielding highly pure MPs for further biotechnological and biomedical applications [32]. Usually, HIC procedures are based on the application of high salt concentrations to promote adsorption upon the exposure of the most hydrophobic residues. However, due to the highly hydrophobic nature of rhSTEAP1-His$_6$, we hypothesized its adsorption with low to medium ionic strength. Indeed, a similar platform was already successfully applied by our research team for the pre-purification of the full length human native STEAP1 using a traditional Butyl-Sepharose matrix and 1.375 M (NH$_4$)$_2$SO$_4$ as binding buffer, dismissing the addition of a detergent or additive, in a negative
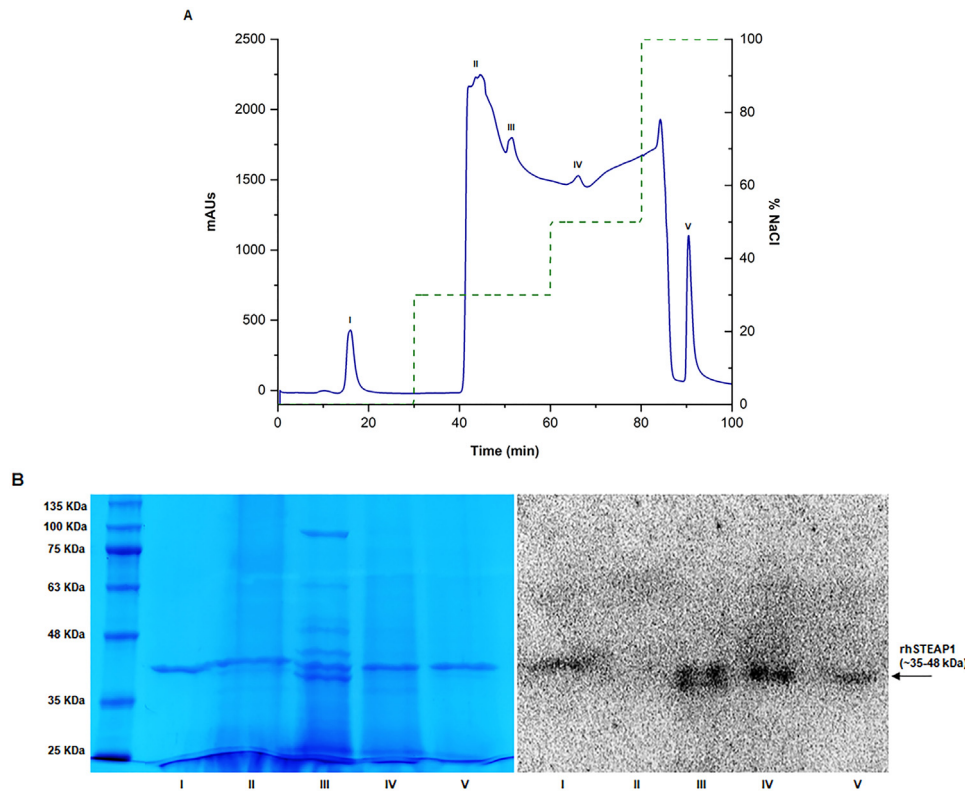
Fig. 4. (A) Chromatographic profile of rhSTEAP1-His$_6$ in a final purification step using HiTrap^{TM} Q FF as an anion-exchanger from the pre-purified fraction with HIC obtained with 10 mM Tris-Base buffer at pH 7.8 + 0.1 % (v/v) NP-40. Blue line represents absorbance at 280 nm. Peak I, adsorption performed at 10 mM Tris-Base buffer at pH 10.0 + 0.1 % (v/v) NP-40 (0.5 mL min^{-1}); Peak II and III, desorption performed at 300 mM NaCl in 10 mM Tris-Base buffer at pH 10.0 + 0.1 % (v/v) NP-40 (1.0 mL min^{-1}); Peak IV, desorption performed at 500 mM NaCl in 10 mM Tris-Base buffer at pH 10.0 + 0.1 % (v/v) NP-40 (1.0 mL min^{-1}); Peak V, desorption performed at 1 M NaCl in 10 mM Tris-Base buffer at pH 7.8 + 0.1 % (v/v) NP-40 (1.0 mL min^{-1}). (B) SDS-PAGE and WB analysis depicted for each peak.

chromatography-like strategy [15]. The selected hydrophobic matrices for this work - HiTrap^{TM} Phenyl HP (5 mL), Butyl-Sepharose^{TM} HP (10 mL), and Octyl-Sepharose^{TM} 4 FF (10 mL) - differ in terms of ligand type and density, hydrophobicity, and dynamic binding capacity. Therefore, we evaluated the influence of these parameters on the chromatographic behavior of rhSTEAP1-His$_6$, under identical binding, elution, and temperature conditions. The results indicated distinct profiles, with rhSTEAP1-His$_6$ elution directly occurring in the flowthrough with 50 mM (NH$_4$)$_2$SO$_4$ in 10 mM Tris-Base buffer at pH 7.8 plus 0.1 % (v/v) NP-40 for Butyl- and Octyl-Sepharose resins, together with heterologous proteins from *K. pastoris* (please see *Supplementary Material* [15,22,24,32-43]). The strength of interaction in HIC is conditioned by the carbon chain length and aromatic content. Common hydrophobic ligands as butyl and octyl groups are linear chain alkanes whose biomolecule retention in HIC increases with the length of the η-alkyl chain and substitution level, despite the tendency of adsorption specificity to decrease [32,40]. On the other hand, the use of aryl ligands or aromatic groups such as phenyl, which present both hydrophobic and aromatic (π-π) interactions, can impact the binding selectivity as well as capacity and strength of retention of the target protein to the chromatographic resin [32,40]. Therefore, the hydrophobicity of Butyl- and Octyl-Sepharose resins together with the lack of capacity to interact with rhSTEAP1-His$_6$ hampered the protein-ligand binding interaction. A proof of concept is the immunologically active monomeric isoform rhSTEAP1-His$_6$ ($\sim$ 35 kDa) totally bind to Phenyl-Sepharose resin and further eluted in 10 mM Tris-Base elution step (Figure 2, Peak II). Interestingly, aggregates of rhSTEAP1-His$_6$ of $\sim$ 48 and 63 kDa directly eluted in the flowthrough (Figure 2, Peak I). This tendency of elution through different peaks is generally related to different adsorption faces or aggregation events, which origin multi-

meric isoforms of rhSTEAP1-His$_6$ upon internal hydrophobic interactions between individual protein units, then reducing the attachment points of the target to Phenyl-Sepharose matrix [41]. Although more data are required, the interaction between STEAP1 counterparts may origin aggregates in which the structural rearrangement hide the exposed hydrophobic intracellular tail, consequently avoiding the bind to the chromatographic matrix. These structural differences could explain the lower salt concentration required for monomeric rhSTEAP1-His$_6$ binding to the Phenyl support instead of high molecular weight forms.

Alternatively, the hexahistidine tag incorporated on rhSTEAP1 construct prompted us to evaluate the adsorption behavior of the target protein obtained from *K. pastoris* crude extracts onto HisTrap^{TM} FF (5 mL) with nickel and cobalt. IMAC has been considered a popular strategy for purification bioprocesses due to its high binding capacity, high efficiency, concentrating power, speed of this technique, and insensitivity to protein folding, ionic strength, chaotropic agents, and detergents [42]. In particular, hexahistidine affinity tags and nickel or cobalt affinity resins are widely used as essential tools in biopharmaceutical research for the isolation of highly pure samples of valuable recombinant MPs [42,43] including dvZip, a zinc transporter [44], and tβ1AR, a G protein coupled receptor-transducing complex [45]. Moreover, our research team already reported a strategy for the chromatographic purification of the peripheral recombinant hexahistidine-tagged membrane-bound Catechol-O-methyltransferase (hMBCOMT-His$_6$) obtained from *K. pastoris* methanol-induced cultures, using an integrated strategy of IMAC as capture step followed by IEX as polishing step [22]. The results were truly interesting once the target enzyme was recovered with superior selectivity and with a higher degree of purity, when compared to other works focused on the biosynthesis and purification of COMT. So, we adapted, optimized,
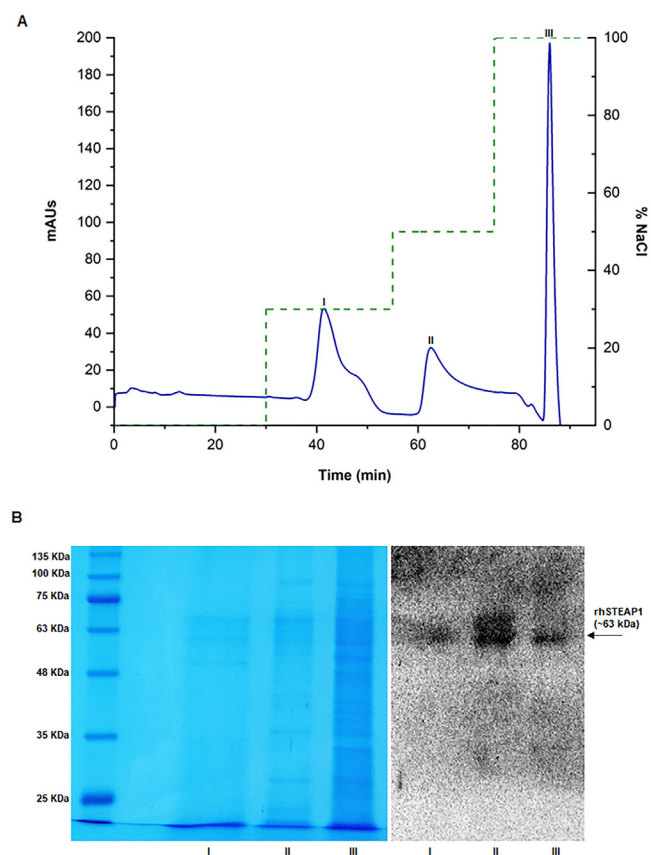
Fig. 5. (A) Chromatographic profile of rhSTEAP1-His$_6$ in a final purification step using HiTrap^{TM} Q FF as an anion-exchanger from the pre-purified fraction with IMAC obtained with 175 mM Imidazole. Blue line represents absorbance at 280 nm. Adsorption performed at 10 mM Tris-Base buffer at pH 10.0 + 0.1 % (v/v) DM (0.5 mL min^{-1}). Peak I, desorption performed at 300 mM NaCl in 10 mM Tris-Base buffer + 0.1 % (v/v) DM (1.0 mL min^{-1}); Peak II, desorption performed at 500 mM NaCl in 10 mM Tris-Base buffer at pH 10.0 + 0.1 % (v/v) NP-40 (1.0 mL min^{-1}); Peak III, desorption performed at 1 M NaCl in 10 mM Tris-Base buffer at pH 7.8 + 0.1 % (v/v) NP-40 (1.0 mL min^{-1}). (B) SDS-PAGE and WB analysis depicted for each peak.

and validated this procedure as an alternative approach for the purification of rhSTEAP1-His$_6$. Accordingly, we loaded rhSTEAP1-His$_6$ samples in cobalt-charged IMAC resin, as it is reported that provides a cleaner sample, a potential advantage for purifying poorly expressed proteins [42]. However, rhSTEAP1-His$_6$ was directly eluted in the flowthrough (Please see *Supplementary Material*). This finding led us to conclude that the tested binding conditions and the initial complexity of the crude extract obtained from *K. pastoris* composed by a significant amount of heterologous and probably interfering proteins did not allow a specific interaction between the hexahistidine-tag of rhSTEAP1 with the cobalt-charged IMAC resin. As a second approach, a nickel-charged IMAC resin was tested in similar experimental conditions, and a partial retention of rhSTEAP1-His$_6$ onto nickel IMAC resin throughout the binding phase (Figure 3B, Peak I) was observed, with the major fraction of the target protein recovered in its immunologically active monomeric isoform of 35 kDa with 175 mM imidazole (Figure 3B, Peak III).

The purity of the rhSTEAP1-His$_6$ samples from both HIC and IMAC was low, considering the amount of co-eluting proteins observed in SDS-PAGE analysis (Figure 2B, Peak II; Figure 3B, Peak III). Based on previous results [22,46], Q-Sepharose was used as a polishing step mainly based on particular rhSTEAP1-His$_6$ basic pI of 9.2 (https://web.expasy.org/compute_pi/, accessed on 11th April 2022), which contrast with the acidic pI of most endogenous *K. pastoris* proteins [21]. When handling pre-purified sample from

HIC, the WB analysis led us to conclude that immunologically active rhSTEAP1-His$_6$ with the expected molecular weight near 35 kDa was preferentially eluted with 300 and 500 mM NaCl both at pH 10.0 (Figure 4B, Peaks III and IV). The tendency for a multipeak elution pattern observed for rhSTEAP1-His$_6$ was also described by us for different MPs, and could be explained by the distinct interacting affinities between amino acids that promote electrostatic interactions and the Q-Sepharose support [22,46]. Interestingly, in the experiment with IMAC pre-purified samples, immunologically active monomeric rhSTEAP1-His$_6$ was almost totally eluted with 500 mM NaCl at pH 10.0 (Figure 5B, Peak II). In both cases, a residual detection of the target protein was verified in the final elution step of 1 M NaCl at pH 7.8 (Figure 4B, Peak V; Figure 5B, Peak III). The combined low ionic strength and basic pH conditions used in the binding phase confers to rhSTEAP1-His$_6$ a negative network charge allowing a direct interaction with the positive-charged Q-Sepharose resin. This behavior proves that the interactions triggered by rhSTEAP1-His$_6$ and Q-Sepharose resin are predominantly stronger via electrostatic moieties. Consequently, the salting-in effected caused by the increased concentration of NaCl led to an impairment in electrostatic free energy and protein-ligand interactions, and consequently to the elution of the target protein [47]. This effect apparently has more impact in the rhSTEAP1-His$_6$ elution instead of the pH manipulation from 10.0 to 7.8 and modification of protein network surface charge. Additionally, this work allowed us to infer that regardless of the initial isolation strategy used (HIC or IMAC), the experimental conditions applied in the polishing step for the purification of a single fraction of monomeric rhSTEAP1-His$_6$ are identical. These facts suggest that the target protein remains fully solubilized in both NP-40 and DM micelles throughout the entire chromatographic bioprocess. Remarkably, the samples recovered with 500 mM NaCl from these two experimental trials showed a high degree of purity with an estimated concentration of 0.90 μg/μL and 0.83 μg/μL, for the HIC and IMAC pre-purified samples (Figure 4B, Peak IV; Figure 5B, Peak II), which represent a final recovery yield of 2.25% and 2.55%, respectively. Despite the apparent reduced protein concentration of the purified rhSTEAP1-His$_6$ fraction, it is important to notice that this was a pioneer study that explore a wide range of typical chromatographic approaches in an attempt to purify the rhSTEAP1-His$_6$ protein, which may demand some exhaustive optimization trials in several steps of a typical recombinant bioprocess to increase the final recovery yield, namely, plasmid construction, expression host, capture and purification technique. Unfortunately, and to our best knowledge, a direct method for the quantification and activity assessment of the STEAP1 protein remains to be explored. The main difficulty is related to the fact that STEAP1 does not have enzymatic activity, which could raise hurdles in the development of a fast and highly sensitive analytic method by High-Performance Liquid Chromatography approaches (e.g., HPLC, UPLC), as our research group previously developed for other membrane protein [48]. Hopefully, the recent cryo-EM structure of STEAP1 reported a potential metalloreductase activity of the protein in reducing metal-ion complexes [5,49]. These prime insights could be an interesting way to explore an alternative procedure for the specific quantification or mass determination of STEAP1 protein. However, the development of this method is dependent on samples with high degree of purity, once other heterologous proteins with similar reducing bioactivity could be interpreted as false positive and impair the results.

Lastly, it is curious to notice that isolated STEAP1 protein appears with different molecular weights of ∼ 48 or 63 kDa, which are also distinct from the molecular weight obtained from the pre-purified samples by HIC or IMAC, with approximately 35 kDa. In a previous work, our team intensively studied and fully optimized the operational and environmental conditions (e.g., time

of fermentation, feeding strategy, and supplementation) for the enhanced biosynthesis of rhSTEAP1-His$_6$ in a mini-bioreactor apparatus [14]. Interestingly, it was confirmed that rhSTEAP1-His$_6$ was produced in three distinct molecular weights of near 35, 48, and 63 kDa, probably as a result of protein aggregation or unspecific interactions, even with the addition of proline, that has a role as stabilizer. Moreover, it was disclosed that the STEAP1 is a functional unit but only upon heterodimeric assemble with other STEAP1 counterparts [5,49]. These data pointed out an innate bias of STEAP1 to interact with surrounding biological compounds. Thus, considering the nature of the protein, its tendency to aggregate, and the distinct environmental conditions throughout chromatographic steps (e.g., type and salt concentration, pH, presence of detergent, resin nature, ligands composition), it is expected that monomeric rhSTEAP1-His$_6$ could aggregate in multimeric complexes, aggregate with particular subunits of other rhSTEAP1-His$_6$, unspecific interact with other proteins or biomolecules, undergo PTMs, or even suffer structural modifications throughout the purification process, looking for a more stable conformation and structural rearrangement. However, more studies are needed to clarify the nature and the mechanisms behind these interaction phenomena.

5. Conclusions

The rhSTEAP1-His$_6$ was sucessfuly expressed in *K. pastoris* minibioreactor cultures in a biologically active and correctly folded conformation [14]. These extracts were solubilized with a wide range of detergents, being NP-40 and DM the most suitable for the extraction and recovery of an active form of rhSTEAP1-His$_6$. The chromatographic purification strategies for the target protein were firstly done by using HIC and IMAC as the capture step, in phenyl-sepharose and nickel-loaded resins. The optimized strategy allowed to selectively isolate the monomeric isoform of rhSTEAP1-His$_6$ from protein aggregates and a considerable amount of *K. pastoris* heterologous impurities. Then, AEX was employed as a final polishing stage for both pre-purified samples, which demonstrated to be highly selective in the elimination of remaining contaminants, and ultimately permitted to obtain a rhSTEAP1-His$_6$ sample with high degree of purity and stability. Interestingly, the polishing strategy was kept reproducible regardless the first purification strategy indicating that the target protein was completely stabilized and encapsulated in both NP-40 and DM micelles. Altogether, the chromatographic approaches here established and implemented for the purification of rhSTEAP1-His$_6$ using a combined strategy between typical hydrophobic or immobilized metal affinity with anion-exchange chromatography allowed to obtain a highly pure fraction of the target from detergent-solubilized *K. pastoris* crude extracts. Also, these experimental procedures could be used as a guide to researchers worldwide as an early approach for the development of purification experiments to other integral or peripheral membrane or soluble proteins. Thus, the experimental research here developed will certainly open doors to explore alternative approaches that might be able to improve the purification yield-related issues to obtain a highly quality protein sample. Ultimately, these strategies constitute the starting point to further structural and biofunctional studies, which may lead to a deeper knowlegde on STEAP1 and the respective development of stronger antagonist biomolecules that can block the oncogenic effects triggered by this protein in cancer patients.

Declaration of Competing Interest

The authors declare no conflict of interest. The funders had no role in the design of the study; in the collection, analyses, or in-

terpretation of data; in the writing of the manuscript, or in the decision to publish the results.

CRediT authorship contribution statement

J Barroca-Ferreira: Investigation, Methodology, Writing – original draft, Writing – review & editing. **AM Gonçalves:** Investigation, Methodology, Writing – review & editing. **MFA Santos:** Data curation, Validation, Visualization, Writing – review & editing. **T Santos-Silva:** Resources, Supervision, Validation, Writing – review & editing. **CJ Maia:** Supervision, Writing – review & editing. **LA Passarinha:** Conceptualization, Funding acquisition, Project administration, Supervision, Validation, Writing – review & editing.

Data Availability

No data was used for the research described in the article.

References

[1] RS Hubert, I Vivanco, E Chen, S Rastegar, K Leong, SC Mitchell, et al., STEAP: a prostate-specific cell-surface antigen highly expressed in human prostate tumors, Proceedings of the Nat. Acad. Sci. 96 (25) (1999) 14523–14528.

[2] J Barroca-Ferreira, J Pais, M Santos, A Goncalves, I Gomes, I Sousa, et al., Targeting STEAP1 protein in human cancer: current trends and future challenges, Curr. Cancer Drug Targets 18 (3) (2018) 222–230.

[3] S-A Esmaeili, F Nejatollahi, A. Sahebkar, Inhibition of intercellular communication between prostate cancer cells by a specific anti-STEAP-1 single chain antibody, Anti-Cancer Agents Med. Chem. (Formerly Current Medicinal Chemistry-Anti-Cancer Agents) 18 (12) (2018) 1674–1679.

[4] TG Grunewald, I Diebold, I Esposito, S Plehm, K Hauer, U Thiel, et al., STEAP1 is associated with the invasive and oxidative stress phenotype of Ewing tumors, Mol. Cancer Res. 10 (1) (2012) 52–65.

[5] W Oosterheert, P. Gros, Cryo-EM structure and potential enzymatic function of human six-transmembrane epithelial antigen of the prostate 1, J. Biol. Chem. 295 (28) (2020) 9502–9512.

[6] K Kim, S Mitra, G Wu, V Berka, J Song, Y Yu, et al., Six-transmembrane epithelial antigen of prostate 1 (STEAP1) has a single b heme and is capable of reducing metal ion complexes and oxygen, Biochemistry 55 (48) (2016) 6673–6684.

[7] S Rocha, J Barroca-Ferreira, L Passarinha, S Socorro, C Maia, in: The Usefulness of STEAP Proteins in Prostate Cancer Clinical Practice, Exon Publications, 2021, pp. 139–153.

[8] JA Carrasquillo, B Fine, N Pandit-Taskar, SM Larson, S Fleming, JJ Fox, et al., Imaging metastatic castration-resistant prostate cancer patients with 89Zr-D-FO-MSTP2109A anti-STEAP1 antibody, J. Nucl. Med. 60 (11) (2019) 1517–1523.

[9] DC Danila, RZ Szmulewitz, U Vaishampayan, CS Higano, AD Baron, HN Gilbert, et al., Phase I Study of DSTP3086S, an antibody-drug conjugate targeting six-transmembrane epithelial antigen of prostate 1, in metastatic castration-resistant prostate cancer, J. Clin. Oncol. 37 (36) (2019) 3518–3527.

[10] T-Y Lin, JA Park, A Long, H-F Guo, N-KV. Cheung, Novel potent anti-STEAP1 bispecific antibody to redirect T cells for cancer immunotherapy, J. Immunother. Cancer 9 (9) (2021).

[11] L Guo, H Xie, Z Zhang, Z Wang, S Peng, Y Niu, et al., Fusion protein vaccine based on Ag85B and STEAP1 induces a protective immune response against prostate cancer, Vaccines 9 (7) (2021) 786.

[12] AK Sendamarai, RS Ohgami, MD Fleming, CM. Lawrence, Structure of the membrane proximal oxidoreductase domain of human Steap3, the dominant ferrire-

ductase of the erythroid transferrin cycle, Proc. Natl. Acad. Sci. 105 (21) (2008) 7410–7415.

[13] W Oosterheert, LS van Bezouwen, RN Rodenburg, J Granneman, F Förster, A Mattevi, et al., Cryo-EM structures of human STEAP4 reveal mechanism of iron (III) reduction, Nat. Commun. 9 (1) (2018) 4337–4346.

[14] D Duarte, J Barroca-Ferreira, A Gonçalves, F Santos, S Rocha, A Pedro, et al., Impact of glycerol feeding profiles on STEAP1 biosynthesis by Komagataella pastoris using a methanol-inducible promoter, Appl. Microbiol. Biotechnol. (2021) 1–14.

[15] J Barroca-Ferreira, P Cruz-Vicente, MF Santos, SM Rocha, T Santos-Silva, CJ Maia, et al., Enhanced stability of detergent-free human native steap1 protein from neoplastic prostate cancer cells upon an innovative isolation procedure, Int. J. Mol. Sci. 22 (18) (2021) 10012.

[16] E Gulezian, C Crivello, J Bednenko, C Zafra, Y Zhang, P Colussi, et al., Membrane protein production and formulation for drug discovery, Trends Pharmacol. Sci. 42 (8) (2021) 657–674.

[17] M Karbalaei, SA Rezaee, H. Farsiani, Pichia pastoris: A highly successful expression system for optimal synthesis of heterologous proteins, J. Cell. Physiol. 235 (9) (2020) 5867–5881.

[18] A Emmerstorfer-Augustin, T Wriessnegger, M Hirz, G Zellnig, H. Pichler, Membrane protein production in yeast: modification of yeast membranes for human membrane protein production, in: Recombinant Protein Production in Yeast, Springer, 2019, pp. 265–285.

[19] A Pedro, D Oppolzer, M Bonifácio, C Maia, J Queiroz, L Passarinha, Evaluation of MutS and Mut+ pichia pastoris strains for membrane-bound catechol-o-methyltransferase biosynthesis, Appl. Biochem. Biotechnol. 175 (8) (2015) 3840–3855.

[20] UK. Laemmli, Cleavage of structural proteins during the assembly of the head of bacteriophage T4, Nature 227 (5259) (1970) 680–685.

[21] C Huang Jr, LM Damasceno, KA Anderson, S Zhang, LJ Old, CA Batt, A proteomic analysis of the Pichia pastoris secretome in methanol-induced cultures, Appl. Microbiol. Biotechnol. 90 (1) (2011) 235–247.

[22] A Pedro, A Gonçalves, J Queiroz, L. Passarinha, Purification of histidine–tagged membrane-bound catechol-o-methyltransferase from detergent-solubilized pichia pastoris membranes, Chromatographia 81 (3) (2018) 425–434.

[23] A Pedro, P Pereira, M Bonifácio, J Queiroz, L Passarinha, Purification of membrane-bound catechol-o-methyltransferase by arginine-affinity chromatography, Chromatographia 78 (21-22) (2015) 1339–1348.

[24] FM Santos, AQ Pedro, RF Soares, R Martins, MJ Bonifácio, JA Queiroz, et al., Performance of hydrophobic interaction ligands for human membrane-bound catechol-O-methyltransferase purification, J. Sep. Sci. 36 (11) (2013) 1693–1702.

[25] V Lantez, I Nikolaidis, M Rechenmann, T Vernet, Noirclerc-Savoye M. Rapid automated detergent screening for the solubilization and purification of membrane proteins and complexes, Eng. Life Sci. 15 (1) (2015) 39–50.

[26] A. Roy, Chapter Three-Membrane Preparation and Solubilization, Methods Enzymol. 557 (2015) 45–56.

[27] A Sadaf, KH Cho, B Byrne, PS. Chae, Amphipathic agents for membrane protein study, Methods Enzymol. 557 (2015) 57–94.

[28] V Kotov, K Bartels, K Veith, I Josts, UKT Subhramanyam, C Günther, et al., High--throughput stability screening for detergent-solubilized membrane proteins, Sci. Rep. 9 (1) (2019) 1–19.

[29] AM Seddon, P Curnow, PJ. Booth, Membrane proteins, lipids and detergents: not just a soap opera, Biochim Biophys Acta Biomembr 1666 (1) (2004) 105–117.

[30] GG. Privé, Detergents for the stabilization and crystallization of membrane proteins, Methods 41 (4) (2007) 388–397.

[31] A Anandan, A. Vrielink, in: Detergents in membrane protein purification and crystallisation. The next generation in membrane protein structure determination, Springer, 2016, pp. 13–28.

[32] CT. Tomaz, in: Hydrophobic interaction chromatography. Liquid Chromatography, Elsevier, 2017, pp. 171–190.

[33] F. Hofmeister, Zur lehre von der wirkung der salze, Archiv für experimentelle Pathologie und Pharmakologie 25 (1) (1888) 1–30.

[34] J. Porath, Salt-promoted adsorption chromatography, J. Chromatogr. A 510 (1990) 47–48.

[35] L Passarinha, M Bonifácio, P Soares-da-Silva, J. Queiroz, A new approach on the purification of recombinant human soluble catechol-O-methyltransferase from an Escherichia coli extract using hydrophobic interaction chromatography, J. Chromatogr. A 1177 (2) (2008) 287–296.

[36] L Passarinha, M Bonifacio, J. Queiroz, Comparative study on the interaction of recombinant human soluble catechol-O-methyltransferase on some hydrophobic adsorbents, Biomed. Chromatogr. 21 (4) (2007) 430–438.

[37] R Hahn, K Deinhofer, C Machold, A. Jungbauer, Hydrophobic interaction chromatography of proteins: II. Binding capacity, recovery and mass transfer properties, J. Chromatogr. B 790 (1-2) (2003) 99–114.

[38] C Machold, K Deinhofer, R Hahn, A. Jungbauer, Hydrophobic interaction chromatography of proteins: I. Comparison of selectivity, J. Chromatogr. A 972 (1) (2002) 3–19.

[39] BF O'Connor, PM. Cummins, in: Hydrophobic Interaction Chromatography. Protein Chromatography, Springer, 2017, pp. 355–363.

[40] KO. Eriksson, Hydrophobic interaction, in: chromatography. Biopharmaceutical Processing, Elsevier, 2018, pp. 401–408.

[41] CL Kielkopf, W Bauer, IL. Urbatsch, Purification of polyhistidine-tagged proteins by immobilized metal affinity chromatography, Cold Spring Harb. Protoc. 2020 (6) (2020) pdb. prot102194.

[42] E Graeber, VM. Korkhov, in: Affinity purification of membrane proteins. Expression, purification, and structural biology of membrane proteins, Springer, 2020, pp. 129–137.

[43] V Riguero, R Clifford, M Dawley, M Dickson, B Gastfriend, C Thompson, et al., Immobilized metal affinity chromatography optimization for poly-histidine tagged proteins, J. Chromatogr. A 1629 (2020) 461505.

[44] Ma C, Gong C. Expression, Purification and characterization of a ZIP family transporter from desulfovibrio vulgaris. The protein journal. 2021;40(5):776-85.

[45] AF Gavriilidou, H Hunziker, D Mayer, Z Vuckovic, DB Veprintsev, R. Zenobi, Insights into the basal activity and activation mechanism of the $\beta 1$ adrenergic receptor using native mass spectrometry, J. Am. Soc. Mass. Spectrom. 30 (3) (2018) 529–537.

[46] F Correia, F Santos, A Pedro, M Bonifácio, J Queiroz, L Passarinha, Recovery of biological active catechol-O-methyltransferase isoforms from Q-sepharose, J. Sep. Sci. 37 (1-2) (2014) 20–29.

[47] A Jungbauer, R. Hahn, Ion-exchange chromatography, Methods Enzymol. 463 (2009) 349–371.

[48] A Pedro, R Soares, D Oppolzer, F Santos, L Rocha, A Gonçalves, et al., An improved HPLC method for quantification of metanephrine with coulometric detection, J. Chromatogrph. Sep. Tech. 5 (2) (2014) 17–24.

[49] W Oosterheert, J Reis, P Gros, A. Mattevi, An elegant four-helical fold in NOX and STEAP enzymes facilitates electron transport across biomembranes—Similar vehicle, different destination, Acc. Chem. Res. 53 (9) (2020) 1969–1980.